Granular Matter (2019) 21:104
https://doi.org/10.1007/s10035-019-0955-x

ORIGINAL PAPER

A review and analysis of granular shear experiments under low effective stress conditions

Xiaohui Cheng[1] · Shize Xiao[1] · Alex Sixie Cao[1,2] · Meiying Hou[3,4]

Received: 8 March 2019

Abstract
The constitutive law for granular materials is governed mainly by the intergranular friction, which depends strongly on the gravitational force or effective isotropic stress. Such experiments are mostly performed with relatively high effective isotropic stress. This fact poses serious limitations on the formulation of a materially objective constitutive model based on experiments performed on earth. This paper analyzes the limited experimental data of shear strength and rheology of granular materials, subject to low effective stress conditions obtained in microgravity μg as well as in 1 g conditions. Results from these experiments show that granular materials may have an extremely high macroscopic peak friction angle and clear nonlinear S-shape non-Bingham fluidity in low effective stress conditions. In this paper, the classical limit equilibrium method is employed, and a rheological constitutive model is used to study experimental data. The limit equilibrium method enables the authors to correlate the bearing capacity of sand foundation with high peak friction angles under varying effective stress conditions. The calibrated analytical solution for the rheological constitutive model under low effective stress conditions, predicts a clear S-shape correlation of the viscous shear stress and shear strain rate. The mutation or inflection point takes place around the in-situ Niigata earthquake shear strain rate. The results of this paper are of great relevance to the assessment of seismic liquefaction hazards of infrastructure on earth.

Keywords Granular material · Low confining pressure · Microgravity · Shearing · Rheology · Liquefaction

1 Introduction

Compared with Newtonian fluids and elastic solids, the microstructure of granular materials and their deformation mechanisms are much more complex. Granular materials exhibit certain solid properties such as possessing confined shear strength, and rheological properties of viscous fluids such as rate dependent behavior of viscous stress. The frictional deformation nature of granular materials causes its macroscopic physical and mechanical properties to be significantly affected by the effective isotropic stress. Effective isotropic stress states in soil mechanics are given directly by confining pressures of the soil. Considering the influence of particle size, particle density and shear rate, we introduce the inertial number I to measure and define isotropic stress states of the material. In general, typical numbers for experiments in soil mechanics are loading rates from 10^{-6} to 10^{-4} s^{-1}, particle sizes around 1 mm and particle density of around 2500 kg/m^3 for granular materials. In this paper, low stress, very low stress and extremely low stress are defined in Table 1, where the effective stress is normalized by a characteristic bulk modulus value of silicon sand (10 Gpa) [1].

The static shear strength and rheological properties in extremely low stress conditions are the fundamental problems of phase transition in such solid and liquid like materials; they are also of great value to the understanding of sand liquefaction and large post-liquefaction deformations in earthquake engineering.

This article is part of the Topical Collection: InMemoriam of Robert P. Behringer.

✉ Meiying Hou
mayhou@iphy.ac.cn

[1] Department of Civil Engineering, Tsinghua University, Beijing, China

[2] Department of Structural Engineering, Norwegian University of Science and Technology (NTNU), Trondheim, Norway

[3] Key Laboratory of Soft Matter Physics, Beijing National Laboratory for Condensed Matter Physics, Institute of Physics, Chinese Academy of Sciences, Beijing, China

[4] Institute of Modern Physics, Chinese Academy of Science, Lanzhou, China

Published online: 13 October 2019

Table 1 Definitions of different stress levels used in this paper

	Effective stress (kPa)	Effective stress in unit of 10 Gpa	Shear rate (s^{-1})	Inertial number
Low stress	1–10	10^{-7}–10^{-6}	10^{-6}–10^{-4}	10^{-9}–10^{-8}
Very low stress	0.01–1	10^{-9}–10^{-7}	10^{-6}–10^{-4}	10^{-9}–10^{-7}
Extremely low stress	<0.01	$<10^{-9}$	10^{-6}–10^{-4}	$>10^{-7}$

Under 1 g condition on earth, it is relatively difficult to perform experiments on materials under extremely low effective isotropic stress conditions. A standard cylindrical test sample for sand commonly used in soil mechanics, is 5 cm in diameter and 10 cm in height. The dry density of sand samples is typically 1600 kg/m^3. In this test sample, the gravity induced vertical stress in the sample is 0 kPa on the sand surface and 1.6 kPa at the bottom of the test cell. The stress is not only unevenly distributed in the vertical direction, but the test sample also needs to be confined by applying horizontal stress of at least several kPa to stabilize it during experiments. These obstacles have made basic research in extremely low stress conditions stagnant for a long time. Shear resistance and rheological properties of granular materials in low effective stress conditions are some of the research fields lacking a great deal of theoretical research.

In the 1980s and 1990s, scientists of the NASA-MGM (National Aeronautics and Space Administration-Mechanics of Granular Materials) project were the first to achieve very low effective stresses in granular materials under μg in a spacecraft [2]. NASA-MGM scientists carried out triaxial shear experiments on the granular material Ottawa Sand, which revealed that sand has a significantly increased macroscopic peak friction angle in very low effective stress conditions. It appears that the microscopic deformation mechanism in granular materials is different from the traditionally thought sliding friction mechanism.

Since the experiments of the NASA-MGM project, physicists and engineers have performed shear and rheological experiments in μg platforms on dense granular materials on two scales: material scale and model scale. Commonly used μg platforms are drop towers or shafts and parabolic flights.

Kobayashi et al. [3] performed experiments on the bearing capacity of sand foundations under varying effective isotropic stress conditions during parabolic flights. The experiments of Kobayashi et al. were quasi-static shear tests of Toyoura sand on model scale. The main results from these experiments show that the shear strength on model scale is heavily influenced by extremely low effective stress conditions. In other words, the bearing capacity of sand is heavily determined by the stress levels. These extremely low effective stress experiments performed in μg provide important data and insight for possible future lunar landing design.

Towhata et al. [4] performed rapid triaxial shear experiments on the rheological properties of dry sand in a drop shaft in Hokkaido, Japan. Combined with results from experiments under 1 g conditions, Towhata et al. confirmed that the sand exhibits complex nonlinear rheological properties under low effective stress conditions.

Scientists from the Institute of Physics in the Chinese Academy of Sciences and Tsinghua University are currently utilizing a drop tower in Beijing to carry out rheological experiments on granular materials under very low stress conditions. Murdoch et al. [5] used a double ring shear apparatus in a parabolic flight experiment to test the rheological properties of glass beads subject to vertical effective isotropic stress of less than 0.15 kPa. In the experiment of Murdoch et al., only the velocity of the glass beads on the top surface was recorded by a high-speed camera. The effects of different effective isotropic stress on the rheological properties of the glass beads were not able to be confirmed.

μg experiments are expensive in addition to difficult preparation and experimental control. Due to this, scientists have also used the density matching method under 1 g condition to reduce the effective stress to 0 kPa. Other methods to reduce the effective stress are based on the increase of pore water pressure in saturated sand samples. The pore water pressure can be increased by using a vibrating table or a cyclic torsion shear device, which will reduce the effective stress to about 5–20 kPa [3, 5]. Many experiments have been performed on material and model scales on granular materials of various densities using such methods. Experiments based on these methods have significant errors:

- the particle density is lower in the density matching method,
- vibration or undrained cyclic shear have high deviations of effective stress generated by gravity in low effective stress conditions by nearly 20%. Extremely low stress conditions cannot be accurately studied.

Towhata et al. [6, 7] performed experiments on the rheological properties of liquefied sand, which is sand under extremely low effective isotropic stress conditions. These experiments were performed with a small-sized shaking table under 1 g condition. The aims were to study sand liquefaction after an earthquake as well as dynamic forces of pipeline and pile foundations in the sand. By using the

shaking table to raise excess pore water pressure of the saturated sand in the model, the total isotropic stress generated by gravity was offset. This caused the sand to enter a liquefied state. In the liquefied state, a buried rod in the sand was pulled horizontally at constant velocity to examine the correlation between the pulling force and the pulling velocity, see Fig. 1.

The measured pulling force was almost constant with a value of only 5 N. Significant nonlinear correlation between the pulling force and velocity was observed. However, the data from the experiments of Towhata et al. were questionable due to the influence of water in the pores and boundary conditions of the rigid sand box on the shaking table.

Motamed et al. [7] performed experiments like the ones by Towhata et al. [6], but on full scale model in the world's largest shaking table "E-Defense" after the experiments of Towhata et al. In the experiments by Motamed et al., the pore water pressure in the front and rear of the rod was accurately measured. The liquid pressure difference was small compared with the total pulling force, which proved the pressure difference was negligible. As such, the rheological properties of granular materials under low effective stress conditions were quantified.

Otake et al. [8] performed another rod pulling experiment like the ones of Towhata et al. and Motamed et al., but with a vertical rod pulled in dense granular suspension. They attempted to reduce the effective stress of the dilute granular material close to zero by density matching method. Subsequently, rheological shear experiments were performed. Unlike the experiments performed in 1 g condition which shows either a slow, logarithmic increase in the mean force in 2D [9] or a roughly independence of the velocity on the mean pulling force in 3D [10], Otake et al. observed complex nonlinear rheological behavior of sand in low effective stress conditions. When the solid fraction of the granular material exceeded 0.555, the pulling force of the cylinder increased sharply. These observations were used as the basis for research on constitutive models in this paper.

In the model experiments of Otake et al., Towhata et al. and Motamed et al., the low effective stress field is uneven and significant influences from lateral boundary conditions need to be considered. More experimental evidence is necessary for the development of the rheological granular constitutive model.

Several macroscopic physical and mechanical continuum models have been established for the rheological properties of granular materials. Granular rheology is usually referred to as the theory describing steady motion of granular materials. Granular materials in this state of motion can be low density dilute flow which is less than loose random packing, or high-density dense flow which is close to the most dense and irregular packing. Its shear stress and strain rate can vary within a range of five to six orders of magnitude and the spatial distribution can also be uneven. In the dense flow, long-range correlation force chains exist that fluidity and elasticity can coexist.

At present, academia has not proposed a unified rheological theory of granular materials that can describe all rheological phenomena of such wide range. Existing theories include Bagnold's rheological model [11] for fast dilute flow, the widely accepted rate-independent CSSM (Critical State Soil Mechanics) model, the rate-dependent viscoelastic plastic model and more [12]. The research group MiDi (Groupement de Recherche Milieux Divisés) [13, 14] in granular physics proposed a macroscopic model of dense granular rheology. The MiDi model uses a dimensionless inertial number I as the core index for connecting micro and macro time scales. The MiDi model is based on Discrete Element Method (DEM) simulations and many granular rheology experiments such as plane shear,

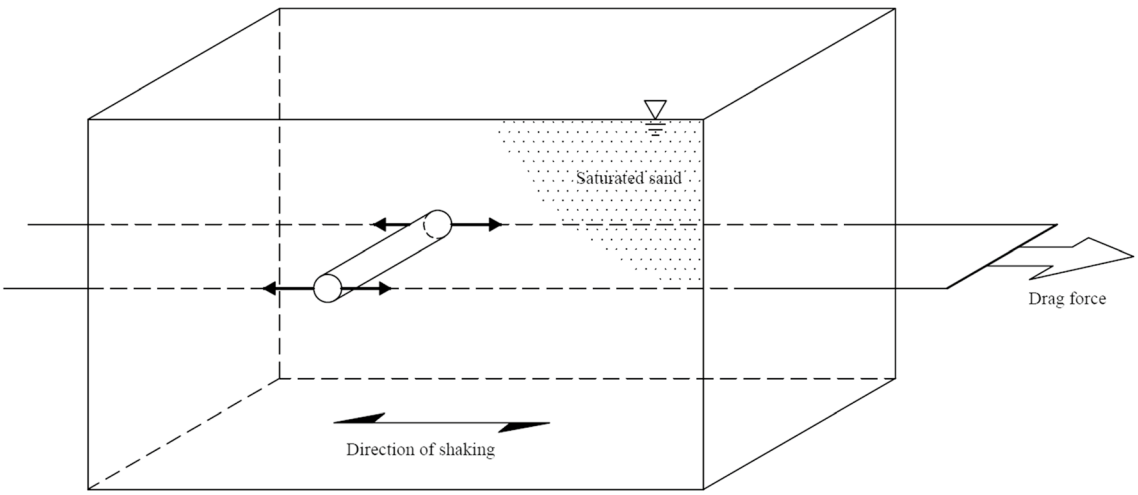

Fig. 1 Sketch of the pulling rod experiments

vertical chute, inclined plane, heap flow, rotating drum and more. It has a relatively simple parametric system and can be easily adopted by other scientists. Jiang and Liu [15] proposed a hydrodynamic granular solid framework using entropy as the core index to describe how granular fluctuation at micro level progressively dissipates into macroscopic heat.

For the quasi-static shear strength of densely or loosely packed granular materials, engineers widely use the Mohr–Coulomb model and Drucker–Prager model as constitutive models for material strength [16]. To consider the influence of unevenness in the stress field and boundary conditions on model scale, several analytical and numerical solutions have been extensively studied and applied. Analytical solutions are widely based on the limit equilibrium method or limit analysis of plasticity, whilst Finite Element Method (FEM) and DEM are widely used for numerical solutions. To the authors' knowledge, there are only a few studies of Smoothed Particle Hydrodynamics (SPH), DEM or large deformation FEM simulations available [8, 17, 18].

In the next sections of this paper, shear strength and rheological triaxial experiments of sand under low effective stress conditions are first outlined. The limit equilibrium method and the MiDi model are then used to verify the applicability of the experiments for describing shear and rheological properties of granular materials under low effective stress conditions. This paper aims to promote the development of unified rheological theory on granular materials and provide basic support for research on seismic liquefaction.

2 Low stress shear experiments

2.1 Shear strength test of dry sand under extremely low stress conditions on material and model levels

Utilizing the μg environment provided by the NASA Space Shuttle, Sture et al. [2] performed six sets of triaxial shear experiments of dry Ottawa sand with two different relative densities. The F1 experiments maintained a relative density of 85% and the F2 experiments maintained a relative density of 65%. In the μg environment of the experiments, the effective isotropic stresses of the experiment samples were reduced to 0.05 kPa, 0.52 kPa and 1.30 kPa as summarized in Table 2.

In the state of maximum shear, Sture and Alshibli et al. found that the experiment samples had significantly higher peak friction and dilatancy angles than under 1 g condition.

Table 2 Results from the experiments performed by Sture et al. [2] in μg

	Confining isotropic stress (kPa)	Relative density (%)	Friction angles (°)
F1 test, set 1	0.05	85	63.4
F1 test, set 2	0.52	85	52.1
F1 test, set 3	1.30	85	53.3
F2 test, set 4	0.05	65	70.0
F2 test, set 5	0.52	65	55.8
F3 test, set 6	1.30	65	47.6

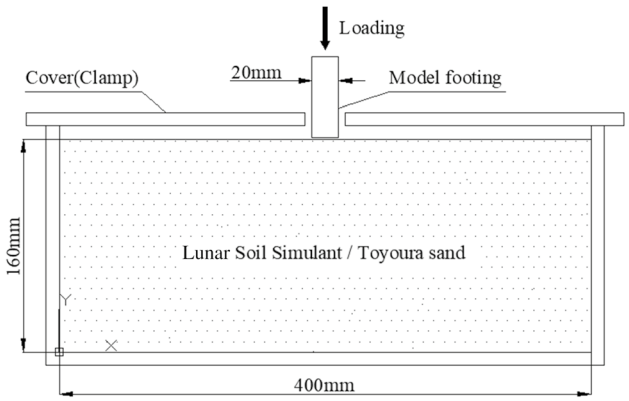

Fig. 2 Sketch of bearing capacity model experiment during parabolic flights [4]

Sato et al. [19] believed that under extremely low isotropic stress conditions, the deformation mechanism would be dominated by the rotation and interlock between particles. The macroscopic behavior of the proposed mechanism of Sato et al. is an increased peak friction angle when the effective isotropic stress decreases. This phenomenon will have far-reaching effects on practical problems such as the ultimate bearing capacity of shallow foundations in space.

Kobayashi et al. [3] performed ultimate bearing capacity experiments on LSS (Lunar Soil Simulant) and Toyoura sand on model scale. The ultimate bearing capacity of the foundation was measured under varying effective isotropic stress conditions. The schematic diagram of the experiment is illustrated in Fig. 2.

The results show that the ultimate bearing capacity of the experiment in low effective isotropic stress conditions is significantly affected by the effective isotropic stress, see Fig. 3.

The settlement curve, ultimate bearing capacity and the residual bearing capacity change significantly with effective isotropic stress conditions for Toyoura sand. The experiments of Kobayashi et al. were performed with non-negligible boundary conditions and uneven effective isotropic stress conditions which may have distorted the results.

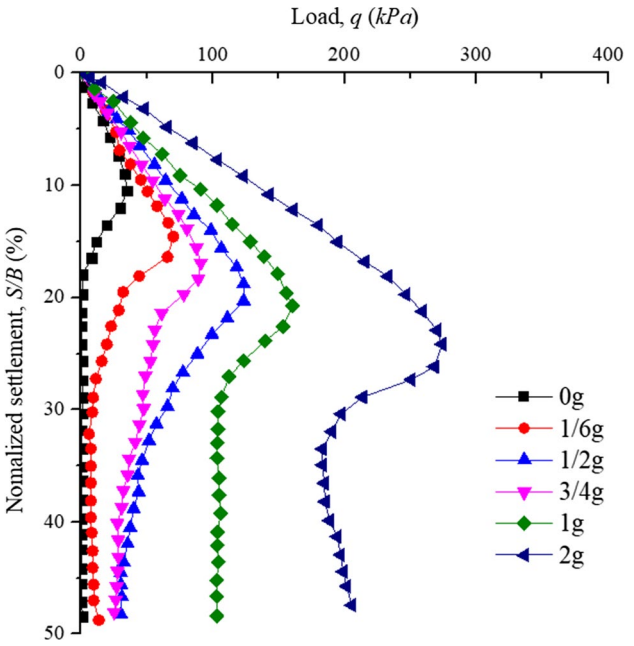

Fig. 3 Bearing capacity of Toyoura sand foundation under varying gravity [4]

The correlation between the peak loads measured by Kobayashi et al. and the peak friction angles measured by NASA-MGM scientists in material level constitutive experiments, is the focus of the next section of this paper.

2.2 Rheological triaxial shear experiments of saturated sand with low effective stress

Gallage et al. [20] performed rheological triaxial shear experiments of saturated sand with low effective stress under 1 g condition. The experiment pre-liquefied the saturated sample by cyclic shear loading to increase the excess pore water pressure in the sample, which reduced the effective isotropic stress of the sample to a level of 5 to 10 kPa. After the sample entered a low effective stress state, stress controlled and stepwise monotonic shear loading was performed. The procedure of the experiment was as follows:

1. In the static state, axial stress is applied suddenly with an increment of $\Delta\sigma = 5$ kPa. The axial stress is kept steady.
2. The sample begins to creep because of the increased axial stress. The shear resistance of the material gradually increases with increased deformation due to creep. The shear rate is gradually reduced.
3. After a period, the shear rate approaches zero and the static strength of the granular material is close to the current load level. The sample returns to a relatively steady state.
4. Repeat steps 1–3.

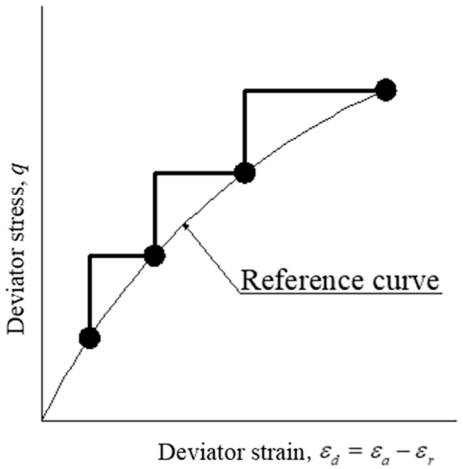

Fig. 4 Sketch of stress controlled and stepwise monotonic shear loading in a low effective rheological triaxial shear test of sand [20]

Figure 4 shows the reference curve Towhata et al. obtained by connecting stress–strain points at the end of each loading step. The reference curve is used to represent the relationship between deviatoric strain ε_d, and deviatoric stress q in the material under quasi-static loading. The deviatoric strain represents shear strain, and deviatoric stress represents the shear stress.

The discrepancy between the measured deviatoric stress and the reference curve can be considered as the stress component from the rheological mechanism called viscous shear stress. Experiments show that there is a positive correlation between viscous shear stress and shear strain rate. Viscous shear stress is also positively correlated with the effective stress and relative density. Due to the influence of gravity under 1 g condition, the effective stress in the experiments of Towhata et al. was still higher than 5 kPa. The stress caused by gravity in the experiment sample cannot be neglected.

Towhata et al. [4] later performed triaxial shear experiments of dry sand in a Japanese drop shaft. Since the time of μg in the drop shaft was limited, the shear strain rate was relatively high. The results from the triaxial shear experiments are illustrated in Fig. 5 in a rheological diagram. Figure 5 show that there is a nonlinear positive correlation between viscous stress and strain rate in the range of low effective stress, which is close to the phase transition point. Independent of sand density, a mutation occurs in the axial strain rate range of about 10^{-4} to 10^{-3} s^{-1}. The typical axial strain rate of the 1965 Niigata Earthquake in Japan was 10^{-3} s^{-1}.

Based on their experimental observations, Towhata et al. tried to use the Bingham rheological model to describe the rheological properties of liquefied sand. However, the Bingham rheological model has some fundamental limitations such as its pressure independency and linearity. These

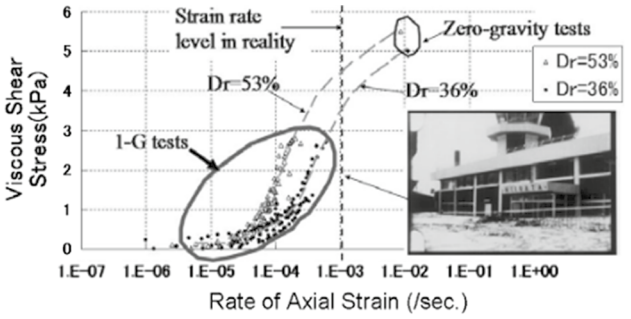

Fig. 5 Summarized viscous shear stress versus axial strain rate correlation for Toyoura sand under low effective stresses [4, 20]

limitations may deem it unfit for the description of the highly nonlinear rheological properties of liquefied sand.

3 Analytical solutions

3.1 Limit equilibrium solutions for the bearing capacity of foundations under varying effective isotropic stress conditions

When a uniform compressive load is applied on the surface of a sand foundation, a gradual development of a plastic failure zone or line will take place. Right before the plastic failure line is complete, the foundation has reached its ultimate bearing capacity. The plastic failure line consists of two linear parts and a logarithmic spiral, as shown in Fig. 6.

The limit equilibrium method is the main theoretical calculation method for solving problems of ultimate bearing capacity of foundations. It was derived after Galileo and Coulomb's work in the 1600 s and 1700 s and plays an important role in engineering.

For two-dimensional problems, the limit equilibrium method generally assumes that the material is a Mohr–Coulomb material, see Eq. 1:

$$\tau_u = c + \sigma_n \tan\phi, \tag{1}$$

where τ_u denotes the ultimate shear strength of the material, ϕ the friction angle and c the cohesion of the material. A Mohr–Coulomb material assumes constant friction angle and cohesion.

For the ultimate bearing capacity of foundations, the classical solution is the Terzaghi solution [21–23] as shown in Eq. 2:

$$p_u = N_q \gamma' D + N_c c + \frac{1}{2} N_\gamma \gamma' B, \tag{2}$$

where N_q, N_c and N_γ are dimensionless bearing capacity coefficients which are functions of the friction angle ϕ. $\gamma' D$ is the vertical effective stress at a depth D from the surface. The expressions of N_q, N_c and N_γ can be found in the Cheng et al. [23].

Equation 2 shows that the ultimate bearing capacity of the Terzaghi solution has contributions from the vertical effective stress $N_q \gamma' D$, cohesive forces between particles $N_c c$, and the gravity $\frac{1}{2} N_\gamma \gamma' B$, where γ' is the effective weight density of the material and B is the width of the foundation. This is illustrated in Fig. 7.

According to the μg shear tests on sand by Sture et al. in the NASA space shuttle, sand has a high peak friction angle under extremely low effective stress conditions. In this paper, the Terzaghi solution is used to study the significance of changing friction angles due to different effective isotropic stress conditions. The peak loads from the bearing capacity experiments of Kobayashi et al. will be used to check if the Terzaghi solution is consistent with data from varying effective isotropic stress conditions.

A general assumption in soil mechanics is that the cohesion of sand is zero, $c = 0$. Following the Terzaghi solution of Eq. 2, the ultimate bearing capacity of the foundation will be zero under zero effective stress. The Terzaghi solution is inconsistent with parabolic flight results from Kobayashi et al. under zero gravity, thus the cohesion is not zero. In view of the particle interlock mechanism proposed by

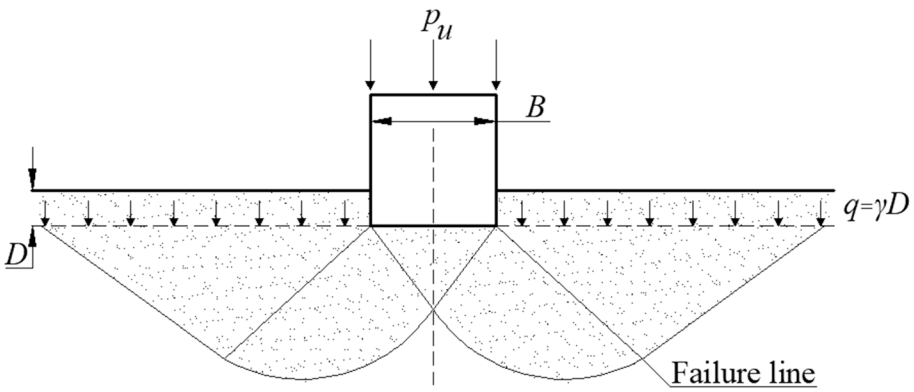

Fig. 6 Sketch of the Terzaghi solution of the ultimate bearing capacity of the foundation

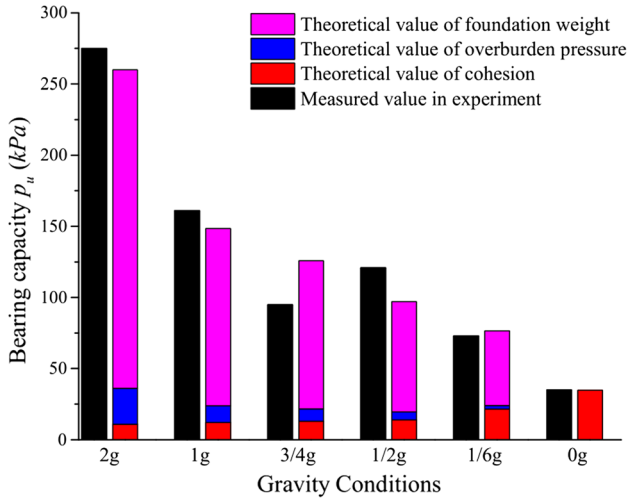

Fig. 7 Comparison of results from parabolic flight experiments and the Terzaghi solution for Toyoura sand with relative density $D_r = 90\%$

NASA-MGM scientists, the Terzaghi solution is used to simulate the ultimate bearing capacity of zero effective stress. This simulation will be used to determine the apparent cohesion of the sand which is assumed to remain unchanged with varying effective stress conditions. The macroscopic friction angle ϕ of the sand will be considered as relative to the effective stress. The ultimate bearing capacity of the model under different effective stress conditions will be simulated by using the Terzaghi solution, which will determine the friction angle at varying effective stress conditions.

The sand used in the experiments of Kobayashi et al. is Toyoura sand with relative density $D_r = 90\%$ which corresponds to a density of $\rho = 1.61\ \mathrm{g/cm^3}$. The macroscopic cohesion of the sand is determined to be $c = 0.05\ \mathrm{kPa}$ by using the Terzaghi solution, the results are illustrated in Fig. 7. The theoretical friction angles under varying effective stress or gravity calculated from the experimental results of Kobayashi et al., can be seen in Table 3.

It should be noted that the stress levels in the experiments of Kobayashi et al. are not uniform. Thus, the theoretical calculation using the same macroscopic friction angle at different locations in the foundation is a simplified method. The calculation results based on the Terzaghi solution, suggest that granular materials may have high peak friction angles under low gravity conditions.

This paper shows that for certain friction angles and cohesions of granular materials, the Terzaghi solution can predict the ultimate bearing capacity of the foundation under varying effective stress conditions.

This paper shows that if the appropriate friction angle and cohesion of granular materials under low stress conditions are selected, the Terzaghi solution can predict the ultimate bearing capacity of the foundation under varying effective stress conditions.

3.2 Simulation of a rheological low effective stress experiment on sand, based on the MiDi model

The Bingham rheological model has great limitations for the nonlinear relationship between the shear strain rate and viscous stress. This was measured in the rheological low effective stress experiment on sand by Towhata et al. In this paper, it is attempted to simulate the rheological properties where the Bingham rheological model is insufficient. This is done by using the MiDi $\mu(I)$ rheological model. The dimensionless inertial number $I = \dot{\gamma} d \sqrt{\frac{\rho}{p'}}$ is used as a core parameter in the MiDi model to describe the relationship between two timescales of dense granular flow. One is the microscopic timescale of particle rearrangement $d\sqrt{\frac{\rho}{p'}}$, which represents the time required for a particle to cross a particle gap under the effective stress p'. The other is the macroscopic timescale of shear deformation $\frac{1}{\dot{\gamma}}$, which is the macroscopic shear deformation rate. The MiDi model assumes that the dense granular flow is incompressible.

There are two macroscopic rate-dependent shear strength parameters included in the MiDi model: the critical friction angle θ_s and the upper limit friction angle θ_1. The critical friction angle θ_s is the minimum friction angle that granular materials need to overcome from the static state to the steady rheological state. The upper limit friction angle θ_1 is defined based on observations from experiments such as inclined plane flow [24].

The MiDi model [14] will degenerate into the pressure dependent Drucker–Prager model when the inertial number is zero, $I = 0$. The critical friction angle θ_s should be rate-independent, and the authors of this paper believe that it is the same angle as the critical state friction angle ϕ defined in soil mechanics. The upper limit friction angle θ_1 is the maximum friction angle when the steady flow velocity of the granular material approaches infinity. In the inclined plane flow experiment, the velocity of the particle flow will accelerate when the angle of the slope is greater than the upper limit friction angle

Table 3 Theoretical friction angles under varying effective stress, calculated from the experimental results of Kobayashi et al.

Effective stress	2 g	1 g	$\frac{3}{4}$g	$\frac{1}{2}$g	$\frac{1}{6}$g	0 g
Friction angle, theoretical	44.5°	45°	45.5°	46°	49°	52°

θ_1. The particle flow cannot enter the steady rheological state in such conditions.

To the authors' knowledge, the MiDi model is used to simulate rheological triaxial phenomena of sand under low stress conditions for the first time. A one-dimensional model can be formulated as Eqs. 3 and 4:

$$\sigma' = p' + \tau \tag{3}$$

$$\tau = \left(\mu_s + \frac{\mu_1 - \mu_s}{\frac{I_0}{I} + 1}\right) p', \tag{4}$$

where σ' is the effective Cauchy stress, p' the effective isotropic stress and τ the shear stress. $\mu_s = \tan\theta_s$ and $\mu_1 = \tan\theta_1$ are the corresponding friction coefficients of the critical friction angle and the upper limit friction angle, respectively. I is the inertial number expressed in Eq. 5, and I_0 is a material parameter reflecting the rheological properties of the granular material.

$$I = \dot{\gamma} d \sqrt{\frac{\rho}{p'}}. \tag{5}$$

The inertial number I is a function of the average particle size d, the dry density ρ, the effective spherical scalar stress of the granular material p' and the macroscopic shear deformation timescale $\frac{1}{\dot{\gamma}}$ of the granular material. The $\frac{1}{\dot{\gamma}}$ can be written in tensor form as Eq. 6:

$$\frac{1}{\dot{\gamma}} = \frac{1}{\sqrt{2 d_t\varepsilon_{ij} d_t\varepsilon_{ij}}}. \tag{6}$$

$\frac{1}{\dot{\gamma}}$ is a function of the strain rate tensor $d_t\varepsilon_{ij}$ which can be written as Eq. 7:

$$d_t\varepsilon_{ij} = d_t e_{ij} + \frac{1}{3} d_t\varepsilon_v \delta_{ij}, \tag{7}$$

where $d_t e_{ij}$ is the deviatoric strain rate tensor and $d_t\varepsilon_v$ is the volumetric strain rate tensor. The volumetric strain rate tensor $d_t\varepsilon_v$ is zero. Since the MiDi model assumes that dense granular flow is incompressible. For conventional triaxial compression, the strain rates in directions x_2 and x_3 are equal $d_t\varepsilon_{22} = d_t\varepsilon_{33}$, which also means that the deviatoric strain rates in x_2 and x_3 directions are equal $d_t e_{22} = d_t e_{33}$.

The MiDi model can be rewritten in three-dimensional form by using stress and strain tensors as Eqs. 8 and 9:

$$\sigma'_{ij} = p'\delta_{ij} + \tau_{ij}, \tag{8}$$

$$\tau_{ij} = \left(\mu_s + \frac{\mu_1 - \mu_s}{\frac{I_0}{I} + 1}\right) \frac{2 d_t e_{ij}}{|\dot{\gamma}|} p', \tag{9}$$

where σ'_{ij} and τ_{ij} now are the effective Cauchy stress tensor and the deviatoric stress tensor, respectively.

In the triaxial experiment, $2\left(d_t e_{11} - d_t e_{33}\right) = \sqrt{3}\dot{\gamma}$ and the deviatoric stress q can be expressed as Eq. 10:

$$q = \sigma'_1 - \sigma'_3 = \left(\mu_s + \frac{\mu_1 - \mu_s}{\frac{I_0}{I} + 1}\right) \frac{\sqrt{3}\dot{\gamma}}{|\dot{\gamma}|} p'. \tag{10}$$

If the quasi-static contribution related to the critical friction angle μ_s from Eq. 10 is subtracted, the viscous contribution of the deviatoric stress can be obtained in Eq. 11:

$$q_v = \left(\frac{\mu_1 - \mu_s}{\frac{I_0}{I} + 1}\right) \frac{\sqrt{3}\dot{\gamma}}{|\dot{\gamma}|} p'. \tag{11}$$

Equation 11 represents the rate-dependent rheological properties of granular materials in the MiDi model, which is the viscous part of the stress.

From the deviatoric stress in Eq. 9, if $|\dot{\gamma}|$ goes towards zero, the granular material satisfies Eq. 12 and the MiDi model degenerates into the Drucker–Prager model:

$$\lim_{|\dot{\gamma}|\to 0} \tau_{ij} \Rightarrow |\tau| = \mu_s p' < \sqrt{\frac{1}{2}\tau_{ij}\tau_{ij}}. \tag{12}$$

The Drucker–Prager model represents the critical state of granular materials under the rate-independent quasi-static state.

In the triaxial experiment conducted by Towhata et al., the discrepancy between the measured deviatoric stress of the sample and the reference curve is the viscous stress of the material. In this paper, the rheological experiments of Yurakucho sand with two relative densities of $D_r = 30.6\%$ and $D_r = 75.0\%$ are simulated. For parameter calibration, the critical friction angle θ_s can be derived directly from the experimental $p' - q$ relationship during critical state. The experiments of Towhata et al. with effective stresses of 3.5 kPa and 15.2 kPa are then used as the benchmark curves for curve-fitting two parameters of the upper limit friction angle θ_1 and the rate dependent material parameter I_0 as shown in Table 4.

This paper uses the MiDi model to simulate the relationship between the strain rate and viscous stress of Yurakucho sand. As shown in Fig. 8, the viscous stress in the sample

Table 4 MiDi model parameters for Yurakucho sand

Relative density D_r (%)	Mean particle size d/mm	θ_s/°	θ_1/°	I_0
30.6	0.24	25	41	0.0001
75.0	0.24	25	46	0.0001

increases with increasing strain rate. The viscous stress gradually reaches a certain limit and is influenced by the effective isotropic stress and relative density of the material. The results from the simulation in Fig. 8 shows that when the deviatoric strain rate ε_d is less than 10^{-3}, the viscous stress q rapidly increases. In the traditional critical state mechanical model, the granular material is however rate-independent.

Towhata et al. summarized the relationship between the axial strain rate and viscous force of sand after performing a series of rheological triaxial experiments on sand. This rheological relationship showed complex nonlinear characteristics and has great relevance for the analysis and prevention of large deformations after earthquake induced ground liquefaction.

Based on the experimental data of Towhata et al. and simulations in this paper, the authors of this paper used the MiDi model to simulate the rheological behavior of the same Yurakucho sand under lower effective stress conditions. A good curve fit was obtained with the material parameters as shown in Table 5, the results are illustrated in Fig. 9.

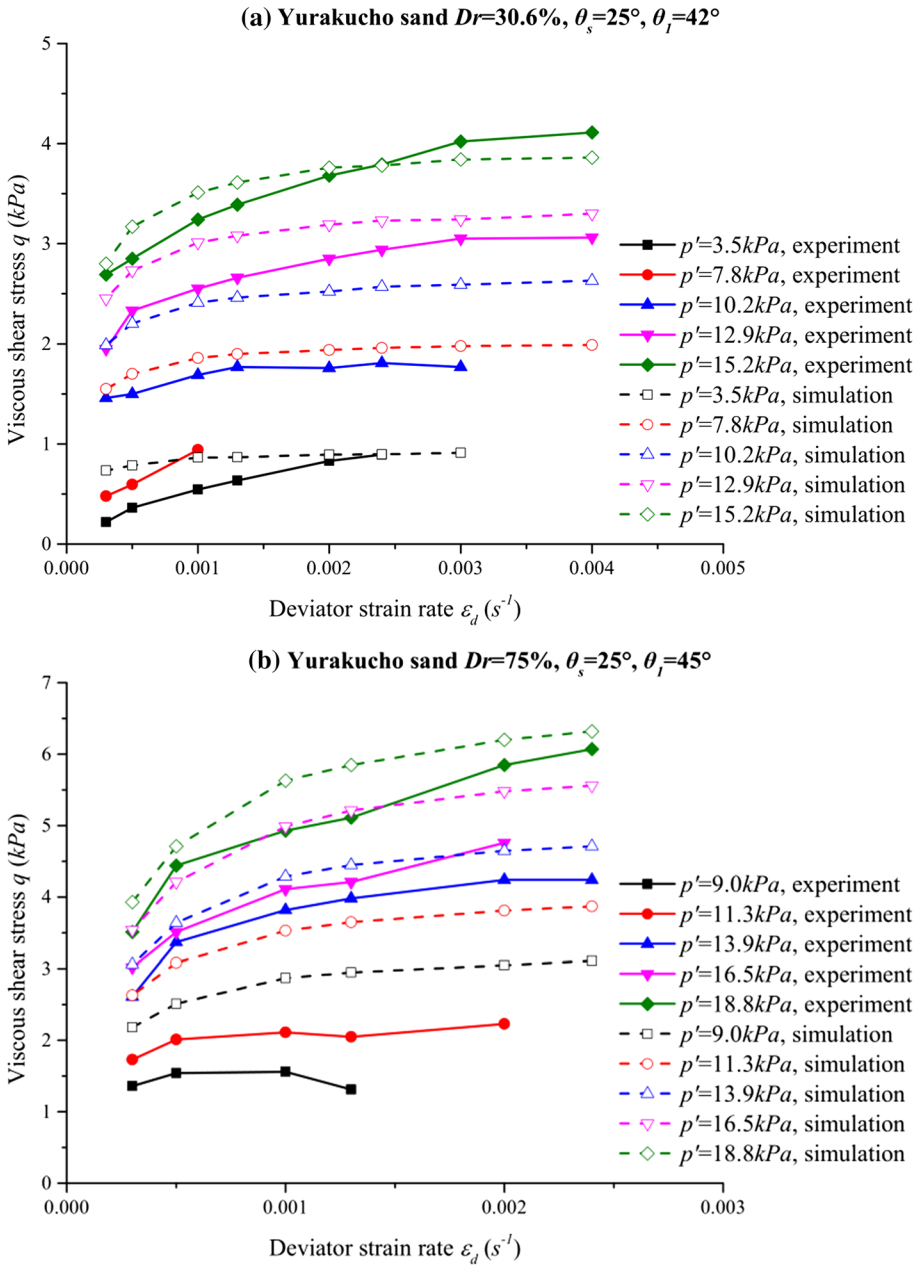

Fig. 8 Simulations of rheological properties of Yurakucho sand by use of the MiDi model

Table 5 MiDi model parameters for Yurakucho sand under lower effective stress conditions

Relative density D_r (%)	Mean particle size d/mm	θ_s/°	θ_1/°	I_0
36	0.24	25	42	0.0001
57	0.24	25	45	0.0001

The correlation curve of viscous stress and the axial strain rate ε_a under effective stress conditions of 1 to 5 kPa, is S-shaped as can be seen from Fig. 9. The viscosity coefficient of the granular material is nonlinearly correlated with the axial strain rate. The S-shaped curve approaches a limit value in case of high axial strain rates. This phenomenon can be compared with the upper limit friction angle observed in the inclined plane granular flow experiment. At the same time, viscous stress is positively correlated with the relative density and the effective stress of the sand. This is consistent with results from the rheological triaxial experiment on sand under low effective stress conditions.

Towhata et al. did not perform experimental measurements near the axial strain rate of 10^{-3} due to limitations under experimental conditions. Viscous shear stresses near the strain rate of 10^{-3} were simulated by the authors of this paper.

4 Conclusions

This paper outlines the importance of studying the shear strength and rheological properties of granular materials under μg and low effective stress conditions. The main conclusions are as follows:

1. The NASA-MGM project in the 1980s, pioneered the use of μg space laboratories to study the basic properties of granular materials. It was followed by experiments on the bearing capacity of sand foundations in PFCs (Parabolic Flight Campaign) and material scale rheological triaxial experiments under 1 g in low effective stress conditions. The latter experiments enriched the experimental dataset, especially for high peak friction angles for granular materials under low effective stresses and non-Bingham pressure dependent rheological properties.
2. The bearing capacity of sand foundations under varying effective stress conditions on PFCs can be considered by the limit equilibrium solution in soil mechanics. Fitting this analytical solution to experimental data can result in significantly increased macroscopic peak friction angle as the effective stress decreases. This is in direct accordance with experimental results of the NASA-MGM project.
3. The rheological triaxial experiments of sand under 1 g condition and low effective stress conditions give a materially objective rheological constitutive law for

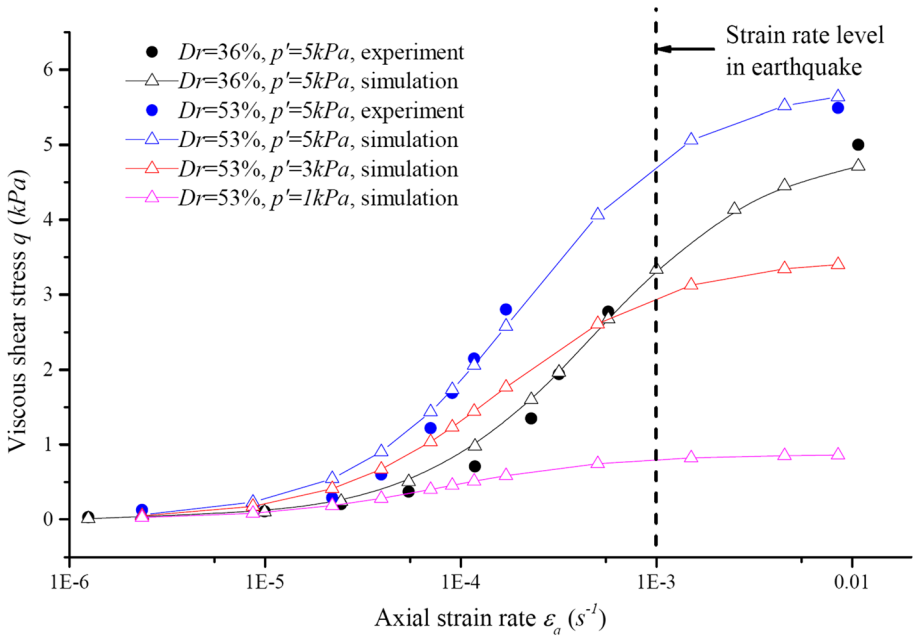

Fig. 9 Simulation of rheological properties of sand near the phase transition point by use of the MiDi model

sand. Compared with the Bingham rheological model, the MiDi rheological constitutive model $\mu(I)$ is based on the inertial number I and five material parameters. These parameters can be used to qualitatively and quantitatively reflect the measured rheological characteristics. The effects of relative density D_r and effective stress on viscous stress are included in the MiDi rheological constitutive model $\mu(I)$. Under quasi-static conditions, the MiDi rheological constitutive model $\mu(I)$ will simplify to the Drucker–Prager model for dense granular matters which is pressure dependent, which is not the case of the Bingham rheological model.

4. The next step will be to continue research into the physical and mechanical behavior of granular materials under μg and low effective stress conditions.

The authors of this paper aim to promote the fundamental research of granular materials in μg environment in space. This research could result in significant technological advances in soil mechanics and earthquake engineering.

Acknowledgement This project is supported by the National Natural Science Foundation of China (Grant Nos. U1738120 and 11474326). The authors would like to thank Qilin Wu for his help on manuscript compiling.

Compliance with ethical standards

Conflict of interest We certify that there is no actual or potential conflict of interest in relation to this article.

References

1. O'Hern, C.S., Silbert, L.E., Liu, A.J., Nagel, S.R.: Jamming at zero temperature and zero applied stress: the epitome of disorder. Phys. Rev. E **68**, 011306 (2003)
2. Sture, S., Costes, N.C., Batiste, S.N., Lankton, M.R., Alshibli, K.A., Jeremic, B., Swanson, R.A., Frank, M.: Mechanics of granular materials at low effective stresses. J. Aerosp. Eng. **11**, 67–72 (1998)
3. Kobayashi, T., Ochiai, H., Suyama, Y., Aoki, S., Yasufuku, N., Omine, K.: Bearing capacity of shallow foundations in a low gravity environment. Soils Found. **49**, 115–134 (2009). https://doi.org/10.3208/sandf.49.115
4. Towhata, I., Anh, T.T.L., Yamada, S., Motamed, R., obayashi, Y.: Zero-gravity triaxial shear tests on mechanical properties of liquefied sand and performance assessment of mitigations against large ground deformation. In: International Conferences on Recent Advances in Geotechnical Earthquake Engineering and Soil Dynamics, Missouri University of Science and Technology, San Diego, California (2010).
5. Murdoch, N., Rozitis, B., Green, S.F., De Lophem, T.L., Michel, P., Losert, W.: Granular shear flow in varying gravitational environments. Granul. Matter **15**, 129–137 (2013)
6. Towhata, I., Vargas-Monge, W., Orense, R.P., Yao, M.: Shaking table tests on subgrade reaction of pipe embedded in sandy liquefied subsoil. Soil Dyn. Earthq. Eng. **18**, 347–361 (1999)
7. Motamed, R., Towhata, I., Honda, T., Tabata, K., Abe, A.: Pile group response to liquefaction-induced lateral spreading: E-defense large shake table test. Soil Dyn. Earthq. Eng. **51**, 35–46 (2013)
8. Otake, K., Guo, S., Matsushima, T.: Experiments of cylinder drag through density-matching particle-fluid mixture and SPH simulation. J. Jpn. Soc. Civ. Eng. Ser. A 2 **72**, I_399–I_407 (2017). https://doi.org/10.2208/jscejam.72.I_399
9. Geng, J., Behringer, R.P.: Slow drag in two-dimensional granular media. Phys. Rev. E **71**, 011302 (2005)
10. Albert, R., Pfeifer, M.A., Barabasi, A.L., Schiffer, P.: Slow drag in a granular medium. Phys. Rev. Lett. **82**, 205 (1999)
11. Bagnold, R.A.: Experiments on gravity-free dispersion of large solid spheres in a Newtonian fluid under shear. Proc. R. Soc. Lond. Ser. A **225**, 49–63 (1954). https://doi.org/10.1098/rspa.1954.0186
12. Roscoe, K.H., Schofield, A.N., Wroth, C.P.: On the yielding of soils. Geotechnique **8**, 22–53 (1958)
13. Forterre, Y., Pouliquen, O.: Flows of dense granular media. Annu. Rev. Fluid Mech. **40**, 1–24 (2008)
14. Brewster, R.: On dense granular flows. Eur. Phys. J. E **14**, 341–365 (2004)
15. Jiang, Y., Liu, M.: Granular solid hydrodynamics. Granul. Matter **11**, 139 (2009)
16. Atkinson, J.H.: The mechanics of engineering soils. Eng. Geol. **11**, 250–250 (1966)
17. Singh, A., Magnanimo, V., Saitoh, K., Luding, S.: The role of gravity or pressure and contact stiffness in granular rheology. New J. Phys. **17**, 043028 (2015)
18. Jeremić, B., Runesson, K., Sture, S.: Finite deformation analysis of geomaterials. Int. J. Numer. Anal. Methods Geomech. **25**, 809–840 (2010)
19. Sato, A., Tanaka, K., Shiote, T., Sasa, K.: Quantification of physical properties of the transitional phenomena in rock from X-ray CT image data. Adv. Comput. Tomogr. Geomater. (2013). https://doi.org/10.1002/9781118557723.ch26
20. Gallage, C.P.K., Towhata, I., Nishimura, S.: Laboratory investigation on rate-dependent properties of sand undergoing low confining effective stress. 地盤工学会論文報告集 **45**, 43 60 (2005). https://doi.org/10.3208/sandf.45.4_43
21. Zhang, X.: Prandtl and Terzaghi bearing capacity formulas of a strip footing solved by slip—line method of plasticity. J. Tianjin Univ. **2**, 92–100 (1987)
22. Terzaghi, K., Terzaghi, K.P., Ralph, B., Terzaghi, K.P., Ralph, B.: Theoretical Soil Mechanics. Wiley, Hoboken (1965)
23. Cheng, G.Y., Qiu, R., Duan, C.: Analytical formula of K. Terzaghi ultimate bearing capacity coefficient under totally coarse foundation base. J. Civ. Aviat. Univ. China. **29**(1), 25–28 (2011)
24. Pouliquen, O.: Scaling laws in granular flows down rough inclined planes. Phys Fluids **11**, 542–548 (1999)